Statistical Methods for Degradation Data with Dynamic Covariates Information and an Application to Outdoor Weathering Data

Yili Hong and Yuanyuan Duan
Department of Statistics
Virginia Tech
Blacksburg, VA 24061

William Q. Meeker
Department of Statistics
Iowa State University
Ames, IA 50011

Deborah L. Stanley and Xiaohong Gu
Materials and Construction Research Division
National Institute of Standards and Technology
Gaithersburg, MD 20899

October 9, 2012

Abstract

Degradation data provide a useful resource for obtaining reliability information for some highly reliable products and systems. In addition to product/system degradation measurements, it is common nowadays to dynamically record product/system usage as well as other life-affecting environmental variables such as load, amount of use, temperature, and humidity. We refer to these variables as dynamic covariate information. In this paper, we introduce a class of models for analyzing degradation data with dynamic covariate information. We use a general path model with individual random effects to describe degradation paths and a vector time series model to describe the covariate process. Shape restricted splines are used to estimate the effects of dynamic covariates on the degradation process. The unknown parameters in the degradation data model and the covariate process model are estimated by using maximum likelihood. We also describe algorithms for computing an estimate of the lifetime distribution induced by the proposed degradation path model. The proposed methods are illustrated with an application for predicting the life of an organic coating in a complicated dynamic environment (i.e., changing UV spectrum and intensity, temperature, and humidity).

Key Words: Covariate process, Environmental conditions, Lifetime prediction, Organic coatings, System health monitoring, Usage history.

1 Introduction

1.1 Background and Motivation

For products and systems with high reliability, it is challenging to do field reliability assessment in a timely manner based only on limited lifetime data. When available, degradation data provide a useful resource for obtaining reliability information because there are degradation measurements for each individual unit in the field before the individual unit fails. For products with degradation driven by usage and environmental conditions, information about these variables can be important for modeling the degradation process. For example, the degradation of organic coatings is primarily driven by Ultraviolet (UV) exposure, while temperature and humidity are other important factors. There are many other more examples that the degradation is driven by usage and environmental variables such as, the loss of light output from an LED array, the decrease of power output of photovoltaic arrays, the corrosion in an oil transportation pipeline, the vibration from a worn bearing in a wind turbine, and the loss of gloss and color of an automobile finish.

The developments in technology allow many systems to collect and transmit massive datasets. It is common nowadays to dynamically record product/system usage and load as well as other environmental variables such as temperature and humidity, which we refer to as dynamic covariate information. For example, even a small device like a power inverter that are used in solar panel arrays can gather and transmit information on the output of power, the ambient temperature and humidity in every few seconds. The availability of such large-scale dynamic data creates many opportunities and challenges.

The dynamic covariate data contain rich information that can be useful for modeling and predicting product reliability. One can expect those units which are heavily used and are used under extreme environments to fail sooner than those units that are less heavily used and are used under normal environmental conditions. Thus it is attractive to incorporate dynamic covariate information into degradation modeling and data analysis, especially when predictions are required for individual units.

Although not all systems will provide degradation data, there are many that will. Examples include power output from a satellite transmitter, power from solar cells, power from voltage inverters, light output from an LED array, number of paper jams per week in a printer/copier, rechargeable battery capacity, etc. The main goal of this paper is to develop general models for analyzing degradation data and dynamic covariate information that are available up to the current time point for a fleet of products. Based on the degradation data model, one can obtain estimates for the lifetime distribution for the product population and for individual units in the field. We use data from an outdoor weathering experiment to illustrate the models

and methods.

1.2 Related Literature

In literature, general path models are commonly used to analyze degradation data (e.g., Lu and Meeker 1993). For a specified failure definition, the cumulative distribution function (cdf) of the lifetime distribution is induced by the parametric model for the degradation paths. Stochastic models are another class of models to analyze degradation data (e.g., Lawless and Crowder 2004). The stochastic model approach assumes that the data are generated from a stochastic process, such as a Wiener process, a gamma process, and an inverse Gaussian process. By the properties of the assumed underlying stochastic process, the cdf of the lifetime distribution can be obtained. Details on parameter estimation for various degradation models are available in Chapter 13 of Bagdonavičius and Nikulin (2001a). Singpurwalla (1995) considered both univariate and multivariate survival models under dynamic environments. Zhou, Serban, and Gebraeel (2011) applied a functional data analysis approach to degradation data modeling.

For degradation data analysis, covariate information and the modeling of covariates are available in several settings such as accelerated repeated-measures degradation tests (e.g., Meeker, Escobar, and Lu 1998, and Bagdonavičius and Nikulin 2001b), accelerated destructive degradation tests (e.g., Escobar et al. 2003), and degradation-test experimental designs (e.g., Joseph and Yu 2006, and Park and Padgett 2006). Gebraeel and Pan (2008) considered a Bayesian linear degradation path model with time varying covariates. Bagdonavičius, Masiulaitytė, and Nikulin (2010) considered a stochastic degradation model with time varying covariates. The time-varying covariates are incorporated into the induced cdf of the degradation process through a cumulative damage model (e.g., see Nelson 2001).

Little work has been done in degradation data modeling that also considers unit-to-unit or temporal variability for covariates. The modeling of the effect of the dynamics on degradation can provide valuable information in several areas. For example, degradation information is important in the area of system health monitoring or condition-based maintenance, where dynamic covariate information is available for continuously monitored systems. Thus, general models for analyzing degradation with dynamic covariate information need to be developed.

1.3 Overview

The rest of the paper is organized as follows. Section 2 introduces a motivating example from the National Institute of Standards and Technology (NIST) outdoor weathering of epoxy coating experiments. Section 2 also introduces the data structure and notation for degradation

data with dynamic covariates. Section 3 proposes a general additive model for incorporating dynamic covariate information into the degradation path model and develops parameter estimation procedures. Section 4 describes parametric models for a multivariate covariate process and the corresponding procedures for parameter estimation. Section 5 develops procedures for failure-time distribution estimation based on the parametric models given in Sections 3 and 4. Section 6 contains some concluding remarks and describes possible areas for future research.

2 Data

2.1 NIST Outdoor Weathering Data

The illustrative application is from the NIST outdoor weathering data. The data were collected in a study of the service life of organic coatings in outdoor environments. Outdoor weathering experiments were carried out in Gaithersburg, MD, from 2002 through 2006. There were 36 specimens placed in outdoor environmental chambers on the roof of a building on the NIST campus, starting at different times of the year. The outdoor temperature, humidity, and Ultraviolet (UV) spectrum and intensity for each unit were recorded automatically by sensors. See Gu et al. (2009) for more details.

A degradation measurement is proportional to the damage to the coating and it was measured periodically for each specimen using FTIR. The degradation measurements were taken at intervals of several days. For illustration, we consider the degradation of aromatic C-O bonds, corresponding to damage number 1250 cm^{-1} on the FTIR spectrum. Figure 1(a) shows nine representative degradation paths from nine specimens, started at different times of the year. The time scale of the degradation measurement, denoted by t, is the time in days since the first measurements. A large part of the variability in these data is due to the varying amount of UV exposure during the nine different periods of time.

For dynamic covariate information, Figures 1b, 1c, and 1d show the daily values of the UV dosage, temperature, and relative humidity (RH), respectively. The time scale for those covariates, denoted by τ, is the time in days since 01 January 2002. Although those covariates are recorded at much more finer resolutions, we aggregated them into daily values for convenience of modeling. Scientifically, the appropriate time scale to model photodegradation should be proportional to the number of photons absorbed into the degrading material. One such quantity is known as dosage. The daily UV dosage at day τ is computed by $\int_{\tau}^{\tau+1} \int_{\lambda_{\min}}^{\lambda_{\max}} E(\zeta, \lambda) \left[1 - e^{A(\lambda)}\right] d\lambda d\zeta$ where the spectral irradiance $E(\zeta, \lambda)$ is the dose (proportional to the number of photons hitting the surface) at time ζ from sun light with wavelength λ, $[1 - e^{A(\lambda)}]$ is the absorbance rate for different wavelengths, and $\lambda_{\min} = 300$ nm and

4

$\lambda_{\max} = 532$ nm give the wavelength limits. Wave lengths above 532 nm are not harmful and wave lengths below 300 nm are generally filtered by atmospheric ozone. The UV spectrum and intensity values were recorded at 12-minute intervals but were aggregated into daily dosage values. For the period between day 598 and day 805, the covariate information is not available because there was no experimental data being collected during that period.

As it can be seen in Figure 1, the environmental covariates show seasonal patterns and also different degrees of variability during different time periods. For example, the UV dosage shows more variability during summer time than during winter time. Due to different starting times, each specimen has its own profile of dynamic covariate information, resulting in different rates of degradation, as we can see from Figure 1(a). For example, those units started in summers initially degraded much more rapidly than those started in winters.

2.2   Notation for the Data

Here we introduce some notation for the degradation data model and the dynamic covariate model. Let $X(t) = [X_1(t), \ldots, X_p(t)]'$ be the usage/environmental information at time t, where p is the number of covariates. Let $\boldsymbol{X}(t) = \{X(s) : 0 \le s \le t\}$ be the history of the covariate process, which records the dynamic information from time 0 to time t.

Suppose there are n units/specimens in the field. For unit i, denote the degradation measurements at time t_{ij} by $y_i(t_{ij})$, $i = 1, \ldots, n, j = 1, \ldots, n_i$, and n_i is the number of time points where degradation measurements were taken. The value of covariate l for unit i at the time s is denoted by $x_{il}(s)$. The history of the covariate process for unit i is denoted by $\boldsymbol{x}_i(t_{in_i}) = \{x_i(s) : 0 \le s \le t_{in_i}\}$ which records the dynamic information from time 0 to time t_{in_i} for unit i. Here $x_i(s) = [x_{i1}(s), \ldots, x_{ip}(s)]'$.

3   Model for a Degradation Path

3.1   General Path Model

Let $\mathcal{D}(t); t > 0$ be the actual degradation path and let

$$y(t) = \mathcal{D}(t) + \epsilon(t) \tag{1}$$

be the degradation measurement at time t. The degradation model implies a degradation path $\mathcal{D}(t)$ for each unit in the population. When the degradation level $\mathcal{D}(t)$ reaches the failure-definition level $\mathcal{D}_f$, a soft failure occurs and we say that the unit has failed. The first crossing time is denoted by $t_{\mathcal{D}}$ and
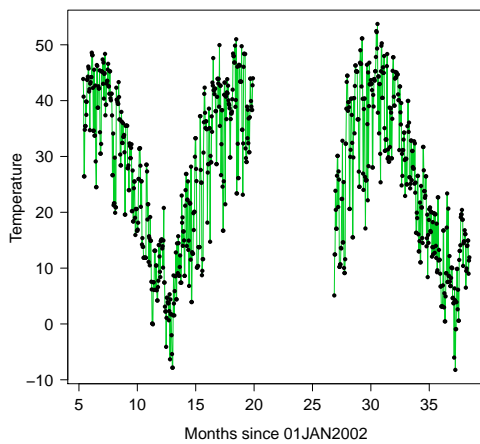
$$t_{\mathcal{D}} = \min\{t : \mathcal{D}(t) \text{ reaches } \mathcal{D}_f\}.$$
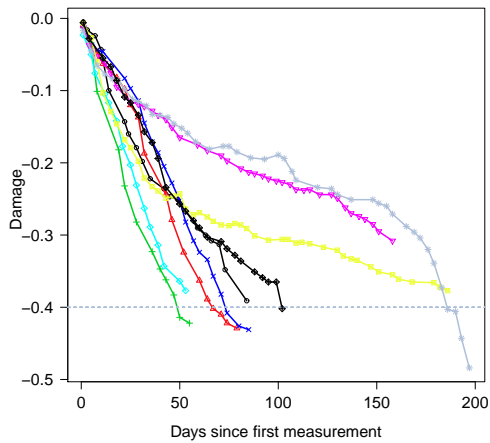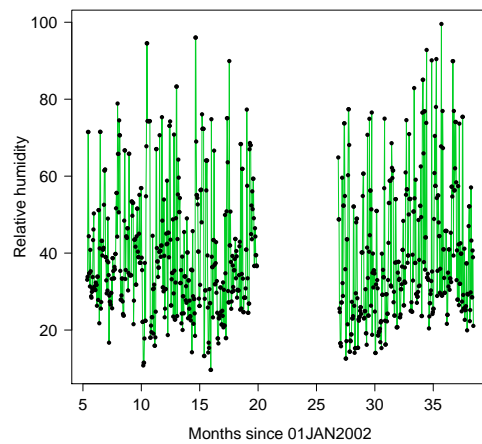
(a) Degradation measurements
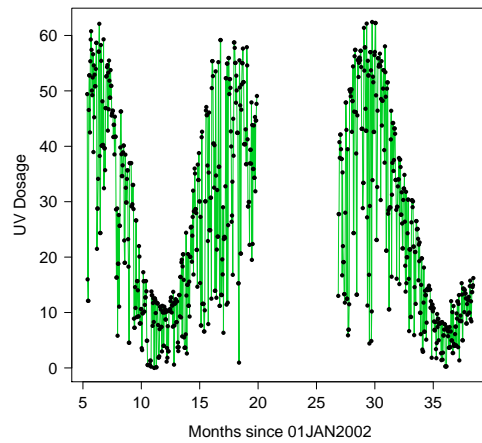
(b) Daily UV dosage

(c) Daily temperature

(d) Daily RH

Figure 1: Plot of nine representative degradation paths and dynamic covariate information (the dots show the daily values, connected by line segments).

The failure-time random variable T is defined as the collection of the failure times $t_{\mathcal{D}}$ for all the units in the population. The cdf of T is $F(t) = \Pr(T \leq t)$. The estimate of $F(t)$ is used for the reliability prediction for the population, which is obtained by using both the degradation measurements and the dynamic covariate information.

3.2 Modeling Degradation Path with Dynamic Covariates

Here we introduce a general additive model to incorporate dynamic covariate information into the degradation path model. In particular, the observed degradation path, conditional on the dynamic covariate information, is modeled as

$$y_i(t_{ij}) = D[t_{ij}; \boldsymbol{x}_i(t_{ij})] + R(t_{ij}; w_i) + \varepsilon_i(t_{ij}). \tag{2}$$

The corresponding model for the actual degradation path is $D[t_{ij}; \boldsymbol{x}_i(t_{ij})] + R(t_{ij}; w_i)$. The first component $D[t_{ij}; \boldsymbol{x}_i(t_{ij})] = \beta_0 + \sum_{l=1}^{p} \int_0^{t_{ij}} f_l[x_{il}(\tau); \beta_l] d\tau$ incorporates the dynamic covariates into the degradation path through a covariate effect transformation function $f(\cdot)$. Here β_0 is the initial level of degradation, and β_l denotes the parameter(s) in covariate effect function $f_l(\cdot)$, $l, l = 1, \ldots, p$. The coefficient vector for the initial degradation and covariate effects is denoted by $\boldsymbol{\beta} = (\beta_0, \beta_1', \ldots, \beta_p')'$. For covariate l, the function $f_l[x_{il}(\tau); \beta_l]$ represents the effect of $x_{il}(\tau)$ at time τ on the degradation process. Thus, $\int_0^t f_l[x_l(\tau); \beta_l] d\tau$ is the cumulative effect of x_l on the degradation process up to time t. This modeling approach is motivated by the cumulative damage model for the accelerated failure time model in Nelson (2001, Chapter 10).

The second component $R(t; w_i)$ is a monotone function of t. An individual random effect w_i is used to account for unit-to-unit variability caused by unobservable factors. A simple but useful form of $R(t_{ij}; w_i)$ is $R(t_{ij}; w_i) = w_{0i} + w_{1i} t_{ij}$ where w_{0i} and w_{1i} are interpreted as individual random effects for the initial degradation and the time trend, respectively. The random effect w_i is modeled by a bivariate normal distribution $N(0, \Sigma_w)$. Let $\boldsymbol{\sigma}_w$ be a general notation for the unique parameters in Σ_w. The third component $\varepsilon_i(t_{ij})$ in (2) is the noise term. In literature, for example, Meeker and Escobar (1998), the $\varepsilon_i(t_{ij})$'s are often modeled to be independent and identically distributed with $N(0, \sigma_\varepsilon^2)$.

3.3 Functional Forms for Covariate Effect $f(\cdot)$

Two alternative approaches are available for choosing the functional form for the covariate effect transformation function $f(\cdot)$. The first approach is based on models motivated by physical, chemical and engineering knowledge. For example, if there is dynamic information on temperature, the Arrhenius relationship (e.g., page 472 of Meeker and Escobar 1998) can sometimes be used to model the effect of temperature on the rate of a degradation process.

When there is not sufficient knowledge about the form of $f(\cdot)$ from physical/engineering knowledge or when such models do not fit the data well, an alternative is to use nonparametric methods. For this approach, the function $f(\cdot)$ is estimated as a linear combination of spline bases. Because most physical variables have a particular relationship with the degradation process (e.g., the degradation rate is increasing as the temperature is increasing), we apply shape restrictions on $f(\cdot)$. To obtain functional forms for $f(\cdot)$ with different shape restrictions (e.g., monotonic increasing, decreasing, or convex), we use shaped-restricted splines described in Meyer (2008).

Here we give a brief introduction to bases for shaped-restricted splines. More details can be found in, for example, Ramsay (1988), and Meyer (2008). Consider a general covariate z with n values $\{z_1, \cdots, z_n\}$. The range of z is denoted by $[z_{\min}, z_{\max}]$. Let $\boldsymbol{z} = (z_1, \cdots, z_n)'$. For regression splines of order h, choose b locations $d_{h+1}, \ldots, d_{h+b}$, and define knots $z_{\min} = d_1 = \cdots = d_h < d_{h+1} < \cdots < d_{h+b} < d_{h+b+1} = \cdots = d_{2h+b} = z_{\max}$. The M-spline basis of order h, denoted by $M_q^{(h)}(z)$, is positive on (d_q, d_{q+h}), zero elsewhere, and has the normalization $\int M_q^{(h)}(z)dz = 1$.

Note that there are $h + b$ M-spline bases of order h, which are given recursively as follows. Order 1 M-splines are the piecewise constant $M_q^{(1)}(z) = \mathbf{1}_{(d_q \leq z < d_{q+1})}(d_{q+1} - d_q)^{-1}$ for $q = 1, \cdots, b+1$ where $\mathbf{1}_{(.)}$ is an indicator function. Order h M-splines are computed recursively by

$$M_q^{(h)}(z) = \frac{h[(z - d_q)M_q^{(h-1)}(z) + (d_{q+h} - z)M_{q+1}^{(h-1)}(z)]}{(h-1)(d_{q+h} - d_q)}\mathbf{1}_{(d_q \leq z < d_{q+h})}$$

for $q = 1, \cdots, b + h$. The I-splines are $\widetilde{I}_q^{(h)}(z) = \int_{z_{\min}}^{x} M_q^{(h)}(u)du$, $q = 1, \ldots, b + h$, for $z \in [z_{\min}, z_{\max}]$. Note that the I-spline bases are monotone increasing functions of z. The I-splines are integrated to obtain C-splines, $\widetilde{C}_q^{(h)}(z) = \int_{z_{\min}}^{z} I_q^{(h)}(u)du$, $q = 1, \ldots, b + h$, for $z \in [z_{\min}, z_{\max}]$. To remove the dependency on the constant spline, the I-splines are regularized by

$$I_q^{(h)}(\boldsymbol{z}) = \widetilde{I}_q^{(h)}(\boldsymbol{z}) - \mathbf{P}_{\{\mathbf{1}\}}[\widetilde{I}_q^{(h)}(\boldsymbol{z})], \quad q = 1, \cdots, b + h \tag{3}$$

where $\mathbf{P}_{\{\mathbf{1}\}}[\widetilde{I}_q^{(h)}(\boldsymbol{z})]$ is the projection of $\widetilde{I}_q^{(h)}(\boldsymbol{z})$ onto the linear space spanned by $\mathbf{1}$. Similarly, to remove the dependency of the constant and identity splines, the C-splines are regularized by

$$C_q^{(h)}(\boldsymbol{z}) = \widetilde{C}_q^{(h)}(\boldsymbol{z}) - \mathbf{P}_{\{\mathbf{1}, \boldsymbol{z}\}}[\widetilde{C}_q^{(h)}(\boldsymbol{z})], \quad q = 1, \cdots, b + h \tag{4}$$

where $\mathbf{P}_{\{\mathbf{1}, \boldsymbol{z}\}}[\widetilde{C}_q^{(h)}(\boldsymbol{z})]$ is the projection of $\widetilde{C}_q^{(h)}(\boldsymbol{z})$ onto the linear space spanned by $\mathbf{1}$ and $\boldsymbol{z}$.

A monotone function is estimated by a linear combination of the basis functions (I-splines) and a constant function. To constrain the estimate to be monotone increasing, the coefficients

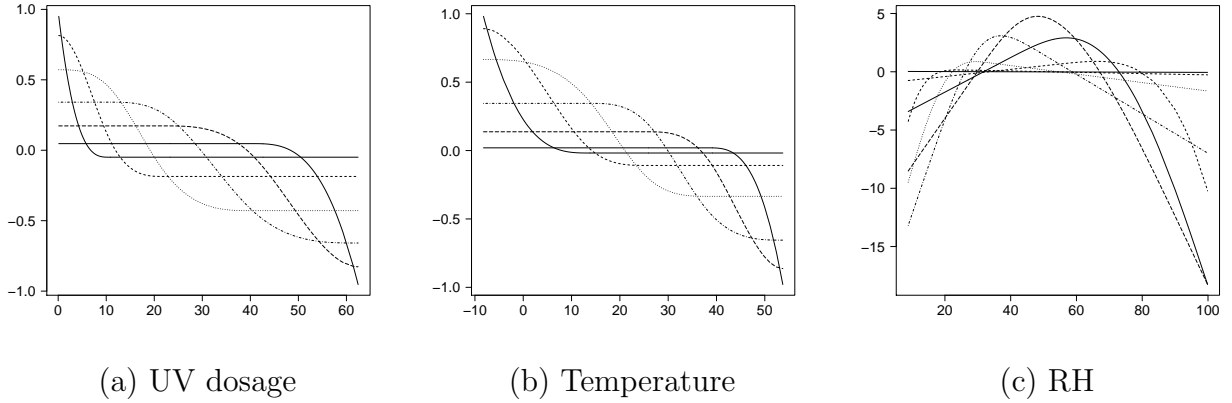| (a) UV dosage | (b) Temperature | (c) RH |

Figure 2: Splines bases for the covariate effects of UV dosage, temperature, and RH.

of the basis functions must be nonnegative (the coefficient of the constant function is not constrained). A convex regression function is estimated using linear combinations of the basis functions (C-splines) with nonnegative coefficients, plus an unrestricted linear combination of the constant function and the identity function $g(x) = x$.

For the outdoor weathering data, the degradation path of the FTIR damage number 1250 cm^{-1} is monotone decreasing. Higher UV dosage or temperature tends to cause larger damage rates. Thus the effects of UV dosage and temperature are constrained to be monotone decreasing in UV dosage and temperature. The effect of RH is constrained to be concave, based on a graphical analysis of the indoor weathering data in Gu et al. (2009) where the RH was controlled (along with other experimental variables) at different levels for serval groups of test units. Figure 2 shows the spline bases for the covariate effects of UV dosage, temperature, and RH. The monotone decreasing splines bases are obtained by using $-I_q^{(h)}(\cdot)$. The concave splines bases are obtained by using $-C_q^{(h)}(\cdot)$. The asymptotically optimal number for b is $b \approx n^{1/(2h+1)}$ (e.g., Meyer 2008). Here the sample size n is taken to be the number of time points where the covariates are recorded. For the weathering data, there are 676 time points. With order 3 polynomial pieces (i.e., $h = 3$), we chose $b = 3$ for the covariates in the weather data. The $b = 3$ locations were chosen as the 0.25, 0.5, and 0.75 sample quantiles of the covariate values.

3.4 Parameter Estimation

Because the degradation data and dynamic covariate process are observed at discrete points in time, the discrete-data version of model (2) is

$$y_i(t_{ij}) = \beta_0 + \sum_{l=1}^{p} \sum_{\tau_{ik} \leq t_{ij}} f_l[x_{il}(\tau_{ik}); \beta_l] + R(t_{ij}; w_i) + \varepsilon_i(t_{ij}). \tag{5}$$

Here $D[t_{ij}; \boldsymbol{x}_i(t_{ij})] = \beta_0 + \sum_{l=1}^{p} \sum_{\tau_{ik} \leq t_{ij}} f_l[x_{il}(\tau_{ik}); \beta_l]$ is still used to denote the discrete-data version of the model. Let $\boldsymbol{\theta}_D = \{\boldsymbol{\beta}, \boldsymbol{\gamma}, \boldsymbol{\sigma}_w, \sigma_\varepsilon\}$ be the collection of unknown parameters. The maximum likelihood (ML) method is used for parameter estimation. Given the observed covariate process, the likelihood is

$$L(\boldsymbol{\theta}_D) = \prod_{i=1}^{n} \int_{w_i} \left[\prod_{t_{ij} \leq t_{in_i}} \frac{1}{\sigma_\varepsilon} \phi \left\{ \frac{B[y_i(t_{ij}); \boldsymbol{x}_i(t_{ij}), w_i]}{\sigma_\varepsilon} \right\} g_{w_i}(w_i; \boldsymbol{\sigma}_w) \right] dw_i \tag{6}$$

where $B[y_i(t_{ij}); \boldsymbol{x}_i(t_{ij}), w_i] = y_i(t_{ij}) - D[t_{ij}; \boldsymbol{x}_i(t_{ij})] - R(t_{ij}; w_i)$, $\phi(\cdot)$ is the probability density function (pdf) of a $N(0, 1)$ distribution, and $g_{w_i}(\cdot)$ is the pdf of a $N(0, \Sigma_w)$ distribution. The ML estimate $\widehat{\boldsymbol{\theta}}_D$ is obtained by finding the value of $\boldsymbol{\theta}_D$ that maximizes (6).

The maximization of (6), in general, is not trivial because numerical methods such as quadrature (e.g., Liu and Pierce 1994) are needed to evaluate the integral in the likelihood function. When shape-restricted splines are used and the random component is modeled as a linear function of w_i, the model in (5) is a linear mixed-effects model with constraints on the parameters. The estimation of the unknown parameters can be done by using the procedure in Davidov and Rosen (2011). For computational efficiency, the constrained quadratic programming used in Davidov and Rosen (2011) can be replaced by the mixed primal-dual bases algorithm used in Fraser and Massam (1989) to solve the generalized least squares problem under constraints.

When shape-restricted splines are used and $R(t_{ij}; w_i) = w_{0i} + w_{1i}t_{ij}$, the model in (5) can be represented by

$$y_i(t_{ij}) = \beta_0 + \sum_{l=1}^{p} \sum_{q=1}^{Q_l} B_{lq}(t_{ij})\beta_{lq} + w_{0i} + w_{1i}t_{ij} + \varepsilon_i(t_{ij}) \tag{7}$$

where $B_{lq}(\cdot)$'s are spline bases, $B_{lq}(t_{ij}) = \sum_{\tau_{ik} \leq t_{ij}} B_{lq}[x_{il}(\tau_{ik})]$, and Q_l is the number of spline bases for covariate l. Let $\boldsymbol{y}_i = (y_{i1}, \ldots, y_{in_i})'$,

$$\boldsymbol{X}_i = \begin{bmatrix} 1 & B_{11}(t_{i1}) & \cdots & B_{1Q_1}(t_{i1}) & \cdots & B_{p1}(t_{i1}) & \cdots & B_{pQ_p}(t_{i1}) \\ \vdots & \vdots & \ddots & \vdots & \ddots & \vdots & \ddots & \vdots \\ 1 & B_{11}(t_{in_i}) & \cdots & B_{1Q_1}(t_{in_i}) & \cdots & B_{p1}(t_{in_i}) & \cdots & B_{pQ_p}(t_{in_i}) \end{bmatrix}, \quad \boldsymbol{Z}_i = \begin{bmatrix} 1 & t_{i1} \\ \vdots & \vdots \\ 1 & t_{in_i} \end{bmatrix},$$

and $\boldsymbol{\varepsilon}_i = [\varepsilon_i(t_{i1}), \ldots, \varepsilon_i(t_{in_i})]'$. Using this notation, the model in (7) can be expressed as

$$\boldsymbol{y}_i = \boldsymbol{X}_i \boldsymbol{\beta} + \boldsymbol{Z}_i w_i + \boldsymbol{\varepsilon}_i.$$

Note that the variance-covariance matrix of $\boldsymbol{y}_i$ is $\Sigma_i = \boldsymbol{Z}_i \Sigma_w \boldsymbol{Z}_i' + \sigma_\epsilon^2 \boldsymbol{I}_{n_i}$ where

$$\Sigma_w = \left[\begin{array}{cc} \sigma_0^2 & \rho\sigma_0\sigma_1 \\ \rho\sigma_0\sigma_1 & \sigma_0^2 \end{array} \right]$$

and $\boldsymbol{I}_{n_i}$ is an $n_i \times n_i$ matrix. Let $\boldsymbol{\sigma}_w = (\sigma_0, \sigma_1, \rho)'$. Some components of $\boldsymbol{\beta}$ are constrained to be nonnegative to produce a shape-restricted covariate effect. Without loss of generality, let $\boldsymbol{\beta} = (\boldsymbol{\beta}_u', \boldsymbol{\beta}_c')'$ where $\boldsymbol{\beta}_u$ and $\boldsymbol{\beta}_c$ represent unconstrained and constrained parameters, respectively.

The estimation algorithm is as follows.

Algorithm 1:

1. Obtain initial values of $\boldsymbol{\sigma}_w$ and σ_ε, which can be done by fitting the unconstrained linear mixed-effects model.

2. Compute $\Sigma_i = \boldsymbol{Z}_i \Sigma_w \boldsymbol{Z}_i' + \sigma_\epsilon^2 \boldsymbol{I}_i$.

3. With Σ_i computed in step 2, use the mixed primal-dual bases algorithm to obtain the estimate of $\boldsymbol{\beta}$ by minimizing $\sum_{i=1}^n (\boldsymbol{y}_i - \boldsymbol{X}_i\boldsymbol{\beta})'\Sigma_i^{-1}(\boldsymbol{y}_i - \boldsymbol{X}_i\boldsymbol{\beta})$ subject to the constraints that the elements of $\boldsymbol{\beta}_c$ are greater than or equal to 0.

4. Fit a linear mixed model to $\widehat{\boldsymbol{\varepsilon}}_i = \boldsymbol{y}_i - \boldsymbol{X}_i\widehat{\boldsymbol{\beta}}$ to obtain updated estimates of $\boldsymbol{\sigma}_w$ and σ_ε.

5. Repeat steps 2 to 4 until convergence.

Making inferences for the constrained ML estimator is not straightforward. Some elements of ML estimate vector may be on the boundary of the parameter space. Although asymptotic theory is available for constrained ML estimator (e.g., Self and Liang 1987), the bootstrap method provides a flexible and easy-to-implement alternative. The residuals and estimated random effects are sampled with replacement to construct the bootstrap version of the data, in which the estimated random effects are adjusted by using the method proposed by Carpenter, Goldstein, and Rasbash (2003). The details of the bootstrap algorithm are described in Appendix A. As pointed out by Morris (2002), the direct resampling (i.e., without appropriate adjustment) of the estimated random effect will result in confidence intervals (CIs) that are too narrow. The estimation procedure in **Algorithm 1** is applied to the bootstrapped data. The resampling process is repeated with a large number of the times (10,000 times here) and CIs can be constructed based on the sample quantiles of the bootstrapped parameter estimates.

Table 1: Parameter estimates and approximate 95% CIs for $\beta_0, \sigma_0, \sigma_1, \rho$ and σ_ε in the degradation path model.

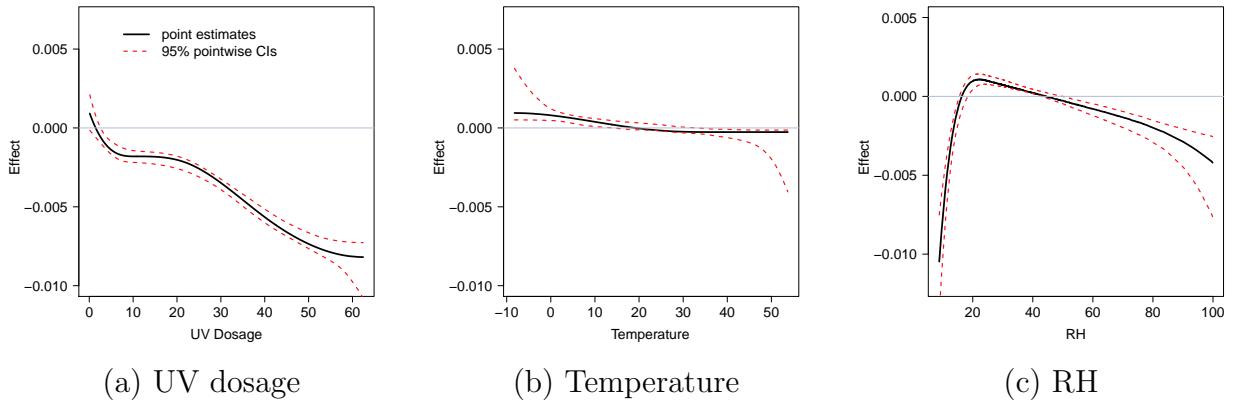| Parameter	Estimate	Standard Error	95% Bootstrap CI	
			Lower	Upper
β_0	-0.04166	0.00398	-0.04971	-0.03419
σ_0	0.02273	0.00319	0.01578	0.02831
σ_1	0.00068	0.00010	0.00046	0.00084
ρ	-0.46114	0.14420	-0.68234	-0.12840
σ_ε	0.01776	0.00053	0.01599	0.01805

(a) UV dosage (b) Temperature (c) RH

Figure 3: Estimated effect functions for UV dosage, temperature, and RH, and the corresponding approximate 95% pointwise CIs.

For the outdoor weathering application, the spline bases shown in Figure 2 are used to fit the effect of UV dosage, temperature, and RH. The parameter estimates are obtained by using the **Algorithm 1**. The estimates and CIs for $\beta_0, \sigma_0, \sigma_1, \rho$, and σ_ε are shown in Table 1. Figure 3 shows the estimated effect functions for UV dosage, temperature and RH, and the corresponding approximate 95% pointwise CIs. Figure 3(a) shows that larger UV dosages lead to more damage. The UV dosage also causes relatively large amounts of damage relative to temperature and RH. Figure 4 shows the plot of degradation measurements and fitted degradation path for the nine representative specimens shown in Figure 1. The figure shows that the general path model fits the degradation data well.
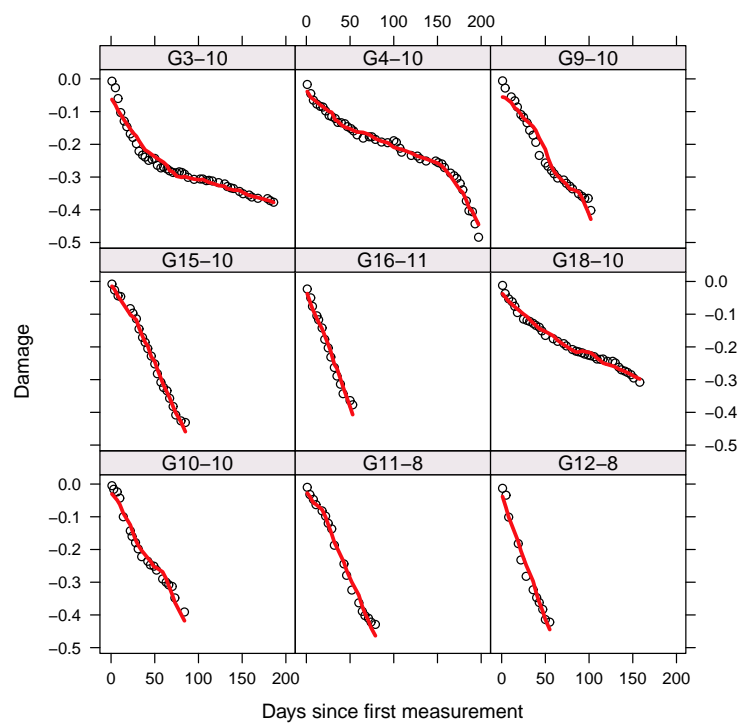
Figure 4: Plot of degradation measurements and fitted degradation path for the nine representative specimens shown in Figure 1.

4 Model for Multivariate Covariate Process

4.1 General Strategy for Covariates Modeling

In order to predict a degradation path into the future, it is necessary to have a parametric model that can adequately predict the covariate process. In general, the following parametric structure for $X(t)$ can be used for each individual unit,

$$X(t) = m(t; \boldsymbol{\eta}) + a(t)$$

where $m(t; \boldsymbol{\eta})$ is the mean function with parameter $\boldsymbol{\eta}$ and some components of $\boldsymbol{\eta}$ can be random to allow for population unit-to-unit (or time period-to-time period in our application) variability for the covariate process. Depending on the application, the parametric form for $m(t; \boldsymbol{\eta})$ can be specified. For example, the environmental temperature of an individual unit can be modeled as

$$X(t) = \text{Trend}(t) + \text{Seasonal}(t) + a(t)$$

where $\text{Trend}(t)$ is the long term trend and $\text{Seasonal}(t)$ is a seasonal periodic term. The error term $a(t)$ is assumed to be a stationary process. In some applications, $a(t)$ for different values of t can be modeled as independently and identically distributed with $\text{N}(0, \Sigma_a)$ where Σ_a is the covariance matrix. The vector autoregressive (VAR) time series models in Reinsel (2003) can be used if more complicated structures are needed for modeling $a(t)$.

4.2 Parametric Models for Covariates for Outdoor Weathering Data

For each application, special modeling effort is needed to capture the unique features in the covariate process. Here we present the modeling of the environmental variables in the outdoor weathering data. Let $x_1(\tau), x_2(\tau)$ and $x_3(\tau)$ be the values of UV dosage, temperature, and RH at time τ, respectively. For these three variables, there is no significant time trend but the seasonal effect is evident. For time series with a seasonal component, combinations of sine and cosine functions are commonly used to capture the seasonal component (e.g., Campbell and Diebold 2005).

Based on initial analysis of the covariates in the weathering data, a single sine function is adequate to describe the mean structure of $x_1(\tau), x_2(\tau)$ and $x_3(\tau)$. There is also a seasonal pattern in the process variance. For example, there is more variability in UV dosage during the summer months than during the winter months. Thus a seasonal component is also added to the variance structure. In particular, the multivariate time series is modeled by

$$\begin{bmatrix} x_1(\tau) \\ x_2(\tau) \\ x_3(\tau) \end{bmatrix} = \begin{bmatrix} \mu_1 + \kappa_1 \sin\left[\frac{2\pi}{365}(\tau - \eta_1)\right] \\ \mu_2 + \kappa_2 \sin\left[\frac{2\pi}{365}(\tau - \eta_2)\right] \\ \mu_3 + \kappa_3 \sin\left[\frac{2\pi}{365}(\tau - \eta_3)\right] \end{bmatrix} + \begin{bmatrix} \left(1 + \nu_1 \left\{1 + \sin\left[\frac{2\pi}{365}(\tau - \varsigma_1)\right]\right\}\right) \varepsilon_1(\tau) \\ \left(1 + \nu_2 \left\{1 + \sin\left[\frac{2\pi}{365}(\tau - \varsigma_2)\right]\right\}\right) \varepsilon_2(\tau) \\ \varepsilon_3(\tau) \end{bmatrix}. \quad (8)$$

The $\sin(\cdot)$ function with a period of 365 days is used to capture the seasonal pattern in the covariates. For the UV dosage and temperature, extra terms are used to capture the nonhomogeneity of variance over time. A likelihood ratio test suggested that the seasonal pattern is not important in the RH variance component. Thus a constant variance component is used for RH.

To further capture the autocorrelation within each covariate and correlation among different covariates, a VAR model is used. In particular, the error term is modeled by

$$\begin{bmatrix} \varepsilon_1(\tau) \\ \varepsilon_2(\tau) \\ \varepsilon_3(\tau) \end{bmatrix} = \Phi_1 \begin{bmatrix} \varepsilon_1(\tau - 1) \\ \varepsilon_2(\tau - 1) \\ \varepsilon_3(\tau - 1) \end{bmatrix} + \Phi_2 \begin{bmatrix} \varepsilon_1(\tau - 2) \\ \varepsilon_2(\tau - 2) \\ \varepsilon_3(\tau - 2) \end{bmatrix} + \begin{bmatrix} e_1(\tau) \\ e_2(\tau) \\ e_3(\tau) \end{bmatrix} \quad (9)$$

where Φ_1 and Φ_2 are matrices of regression coefficients, and $[e_1(\tau), e_2(\tau), e_3(\tau)]' \sim \mathrm{N}(0, \Sigma_e)$ are multivariate normal error terms that are independent over time. Here Σ_e is the covariance matrix for the error terms. For the weathering example, the model fitting suggested that this second order VAR model is adequate.

4.3 Parameter Estimation

The estimation of the parameters in models (8) and (9) is done in two steps. In the first step, ML estimation is used to remove the seasonal trends in the mean and variance structures. Then the residuals are obtained. The ML method is used to obtain the parameter estimates for the model in (8). One needs to program the likelihood function and then use an optimization algorithm (e.g., `optim()` function in R 2012) to maximize. The estimates of the parameters and corresponding CIs for the covariate process model in (8) are listed in Table 2. We used a simple percentile bootstrap approach to obtain CIs. Figure 5 shows the fitted mean structure, estimated error terms, and the estimated standard deviation (SD) of the error term for UV dosage, temperature, and RH. The figure shows that model (8) adequately fits the mean and variance structure for UV dosage, temperature and RH data.

In the second step, ML estimation is used to fit the VAR model to the residuals. The computing of the parameter estimates uses multivariate least squares (e.g., Lütkepohl 2005, Chapter 3), which is computationally efficient. The estimates of Φ_1, Φ_2 and Σ_e are as follows (the subscripts are the corresponding standard errors),

$$\Phi_1 = \begin{pmatrix} 0.582 \, _{0.041} & 0.020 \, _{0.035} & 0.020 \, _{0.011} \\ 0.095 \, _{0.061} & 0.634 \, _{0.051} & 0.018 \, _{0.017} \\ -0.070 \, _{0.195} & -0.046 \, _{0.166} & 0.594 \, _{0.054} \end{pmatrix},$$

$$\Phi_2 = \begin{pmatrix} -0.109 \, _{0.041} & -0.019 \, _{0.034} & -0.013 \, _{0.011} \\ -0.106 \, _{0.061} & 0.030 \, _{0.051} & 0.015 \, _{0.017} \\ 0.388 \, _{0.200} & -0.108 \, _{0.165} & -0.112 \, _{0.054} \end{pmatrix},$$

and

$$\Sigma_e = \begin{pmatrix} 8.870 \, _{1.346} & 4.081 \, _{0.724} & -20.073 \, _{2.380} \\ 4.081 \, _{0.732} & 19.178 \, _{2.688} & -43.636 \, _{4.357} \\ -20.073 \, _{2.380} & -43.636 \, _{4.357} & 200.960 \, _{13.618} \end{pmatrix}.$$

The standard errors of the parameter estimates of Φ_1, Φ_2 and Σ are also obtained by using the bootstrap method. The bootstrap is done by sampling the estimated error term $[e_1(\tau), e_2(\tau), e_3(\tau)]'$ with replacement and then using the parametric models in (8) and (9) to obtain a bootstrap version of the covariate data. The bootstrap version of the parameter estimates are obtained by using the two-step approach. The above process is repeated with a large number of times (e.g., 10,000) to obtain the bootstrap distribution of parameter estimators.

We also examined the autocorrelation function (ACF) of the estimated $[e_1(\tau), e_2(\tau), e_3(\tau)]'$ to check the assumption of the VAR model. The ACF functions of the time series residuals showed no evidence of autocorrelation. Thus the VAR(2) model provides an adequate description of the residuals.

5 Failure-time Distribution Estimation

## 5.1 Failure-time Distribution for the Population

The failure-time distribution provides the reliability information for an unobserved population. We use $\boldsymbol{\theta}_D$ and $\boldsymbol{\theta}_X$ to denote the unknown parameters in the degradation model and covariate process model, respectively. Let $\boldsymbol{\theta} = \{\boldsymbol{\theta}_D, \boldsymbol{\theta}_X\}$. The model for the actual path is $D[t; \boldsymbol{X}(\infty)] + R(t; w)$. Given the covariate process $\boldsymbol{X}(\infty) = \boldsymbol{x}(\infty)$ and the individual random effect w, the degradation path is deterministic. The first crossing (failure) time $t_{\mathcal{D}}$ for a particular unit can be obtained. That is

$$t_{\mathcal{D}} = \min\{t : D[t; \boldsymbol{x}(\infty)] + R(t; w) = \mathcal{D}_f\}. \tag{10}$$

Thus the first crossing time $t_{\mathcal{D}}$ is a function of $\mathcal{D}_f$, $\boldsymbol{x}(\infty)$, and w. Numerical methods are often needed to solve t_D from (10). Because $\boldsymbol{X}(\infty)$ and w are random, the first crossing
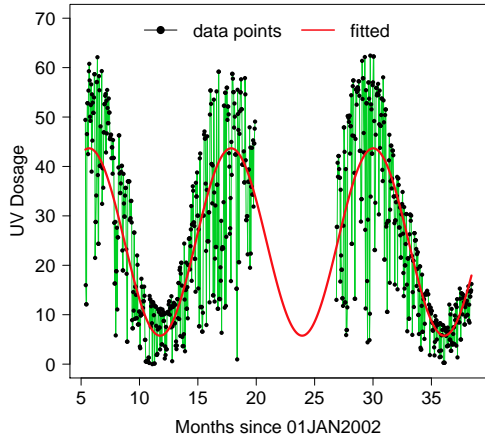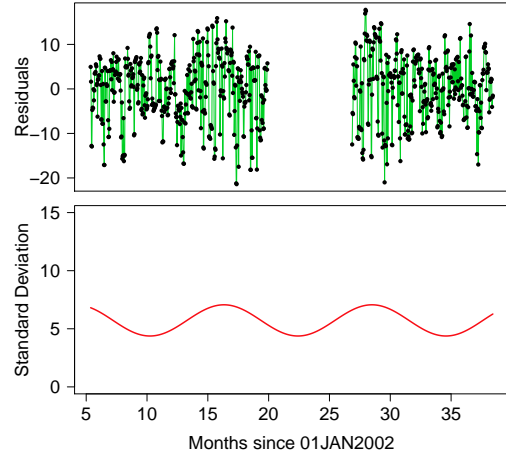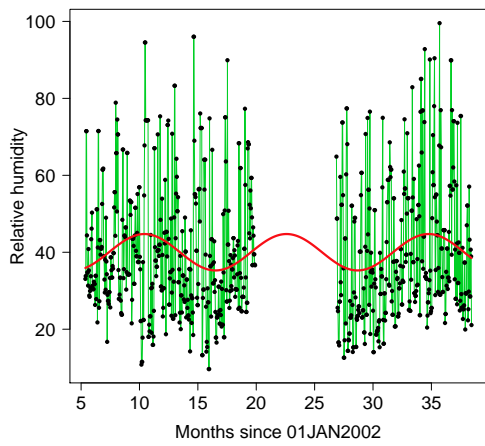
(a)Daily UV dosage
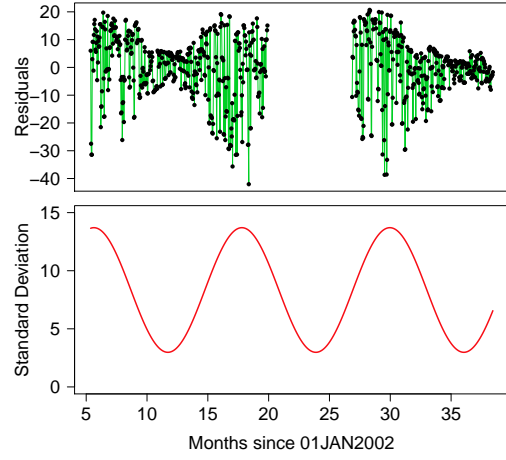
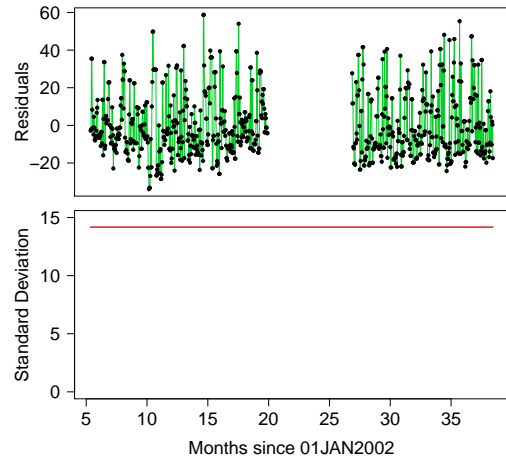(b) UV dosage residuals and estimated SD
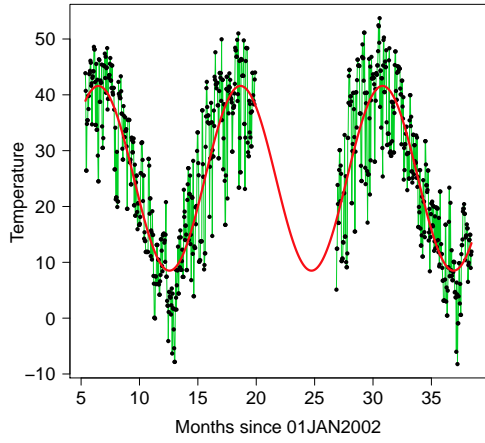
(c) Daily average temperature

(d) Temperature residuals and estimated SD

(e) Daily average RH

(f) RH residuals and estimated SD

Figure 5: The fitted mean and variance structures for UV dosage, temperature and RH.

Table 2: Parameter estimates and corresponding 95% bootstrap CIs for the parameters of the covariate process model in (8).

Covariate	Parameter	Estimate	Standard Error	95% Bootstrap CI Lower	95% Bootstrap CI Upper
UV Dosage	μ_1	24.71	0.58	23.58	25.84
	κ_1	18.95	0.70	17.58	20.35
	η_1	79.24	2.07	75.21	83.34
	ς_1	77.69	3.69	70.43	84.93
	ν_1	1.80	0.24	1.41	2.37
Temperature	μ_2	25.05	0.52	24.04	26.08
	κ_2	16.54	0.69	15.18	17.93
	η_2	103.19	2.67	97.99	108.46
	ς_1	33.53	13.71	8.14	62.41
	ν_2	0.31	0.09	0.16	0.52
RH	μ_3	40.01	1.02	38.02	41.96
	κ_3	-4.73	1.59	-7.67	-1.05
	η_3	39.00	19.23	8.29	80.58

time (i.e., the failure-time of the product), denoted by T, is a random variable. The cdf of $T = T[\mathcal{D}_f, \boldsymbol{X}(\infty), w]$ is

$$F(t; \boldsymbol{\theta}) = \mathbf{E}_{\boldsymbol{X}(\infty)} \mathbf{E}_w \Pr \{ T[\mathcal{D}_f, \boldsymbol{X}(\infty), w] \le t \}, \quad t > 0. \tag{11}$$

In most situations, there is no explicit form for $F(t; \boldsymbol{\theta})$ and it has to be computed by using numerical methods or Monte Carlo simulation.

Substituting $\widehat{\boldsymbol{\theta}}$ into $F(t; \boldsymbol{\theta})$ in (11), one obtains an estimate of the cdf. Because an explicit form for $F(t; \widehat{\boldsymbol{\theta}})$ is, in general, not available, a simulation approach is used to evaluate $F(t; \widehat{\boldsymbol{\theta}})$. The following algorithm is used for computing $F(t; \widehat{\boldsymbol{\theta}})$.

Algorithm 2:

1. Simulate the covariate process with the parameter equal to $\widehat{\boldsymbol{\theta}}_X$.

2. Simulate the random effect w from $\mathrm{N}(0, \Sigma_w)$ with the parameter equal to $\widehat{\boldsymbol{\theta}}_D$.

3. Compute the simulated degradation path $D[t; \boldsymbol{X}(\infty)] + R(t; w)$ with the simulated covariate process and random effect.

4. Given the simulated degradation path, compute the failure-time $t_{\mathcal{D}}$ by solving (10).

5. Repeat the above steps 1 to 4 B times (e.g., $B = 10,000$) to obtain the simulated failure-times $t_{\mathcal{D}}^b, b = 1, \ldots, B$ where B is chosen large enough to provide sufficient precision. The

estimate of $F(t; \boldsymbol{\theta})$ is obtained by $F(t; \widehat{\boldsymbol{\theta}}) = B^{-1} \sum_{b=1}^{B} \mathbf{1}_{(t_{\mathcal{D}}^b \leq t)}$ where $\mathbf{1}_{(.)}$ is an indicator function.

The CIs for the cdf can be obtained as follows. Because the bootstrap parameters $\widehat{\boldsymbol{\theta}}$ are obtained in previous sections, one needs to repeat **Algorithm 2** for each set of bootstrap version of parameter estimates. The pointwise CIs for the cdf are then obtained as the sample quantiles of the bootstrap estimates of $F(t; \boldsymbol{\theta})$. If the focus is on an individual unit, **Algorithm 2** can also be used to obtain the estimates for the cdf of an individual unit.

The manner in which our model and inference procedures would be used in applications will depend on relationship between the units of interest and the processes generating the covariates that will affect the degradation processes. Some example scenarios include the following.

1. In some applications all units in the population will be subject to different realizations of a covariate processes that could be adequately modeled as independent (but not identically distributed) from unit to unit (location to location). For example, when considering the loss of light output from LED lights in household, the usage history (the covariate) are different but can be considered to be independent from household to household.

2. Similar to the groups of units in the weathering experiment, one might be interested in estimating the failure time distribution of a population of units that are all subject to the same realization from the covariate processes. For example, when consider the power output decrease of solar panels installed at one location (e.g., one power plant), the environmental variables such as temperature and humidity can be considered to be the same for each unit in the field.

3. Similar to the overall weathering experiment, one might be interested in groups of units put into service at various points in time (known as staggered entry) so that the groups are subject to different parts of the same covariate process. The illustrative outdoor weathering example in this paper falls into this category.

5.2 Application to the Epoxy Degradation Example

To illustrate the use of our methods, we use the outdoor weathering setting and assume that there is a hypothetical population with infinite size and that units randomly enter service, according to a uniform distribution, between day 161 and day 190. Each unit has its own independent realization of the covariate processes, from the observed processes in the experiment. Figure 6 shows the estimated cdf and the corresponding 95% pointwise CIs for this

hypothetical population. Most of the units in the population fail between 50 days to 150 days after they are put into service. Similar results can be obtained for the cdf of an individual unit (e.g., a unit started at day 161).

For the NIST outdoor weathering data, we also checked how well the failure-time model fits the observed failure times. For the weathering data, we use a failure threshold $\mathcal{D}_f = -0.4$. Generally, this would be chosen to be the level of degradation at which the performance of the coating would not be acceptable (e.g., the level at which there would be customer perceivable loss of gloss or color). According to this definition, there were 17 failures out of 36 units that were put into experiments at different times from 2002 to 2006. The other 19 units survived.

Figure 7 shows the estimated expected number of failures and corresponding 95% pointwise CIs versus the observed number of failures as a function of time for the 36 specimens in the outdoor weathering data. The dots show the observed number of failures as a function of time. The estimated expected number of events is computed based on the estimated degradation path and covariate process models. For the periods from day 0 to day 597 and from day 806 to day 1153, the covariate processes for the weathering data were already observed, we treat the covariates as fixed when we compute the estimated expected number of failures. For those periods that between day 598 to day 805 and after day 1153, realizations of the covariate process are needed to compute the estimated expected number of events. Thus multiple realizations of the covariate processes were simulated and the results were averaged for those periods. The results in Figure 7 show that the estimated expected number of failures track the observed number of failures well except that there is an abrupt jump around day 50 in the observed number of failures.

5.3 Distribution of Remaining Life for Individual Units

Given the observed degradation path and the covariate process up to time t_{in_i} for individual i, the distribution of the remaining failure-time is needed in some applications. In particular, the conditional distribution for individual with $\boldsymbol{X}_i(t_{in_i}) = \boldsymbol{x}_i(t_{in_i})$ is

$$\rho_i(s; \boldsymbol{\theta}) = \mathbf{E}_{\boldsymbol{X}_i(\infty)|\boldsymbol{X}_i(t_{in_i})=\boldsymbol{x}_i(t_{in_i})}\mathbf{E}_w \Pr\left\{T[\mathcal{D}_f, \boldsymbol{X}(\infty), w] \le t_{in_i} + s | T > t_{in_i}\right\}, s > 0.$$

Here $\rho_i(s; \boldsymbol{\theta})$ gives the failure probability at a future time, conditional on $\boldsymbol{X}_i(t_{in_i}) = \boldsymbol{x}_i(t_{in_i})$. Similar algorithms can be used to evaluate the conditional distribution $\rho_i(s; \widehat{\boldsymbol{\theta}})$ for individual i and the corresponding pointwise CIs. The difference is that the future degradation path and the covariate process are conditional on $\boldsymbol{x}_i(t_{in_i})$ and the degradation measurements that have been observed up to time t_{in_i}.

For illustration, we consider the specimen labeled "G18-10" with age of 158 days by the end of exposure. The observed degradation level for G18-10 had not reached $\mathcal{D}_f = -0.4$ after
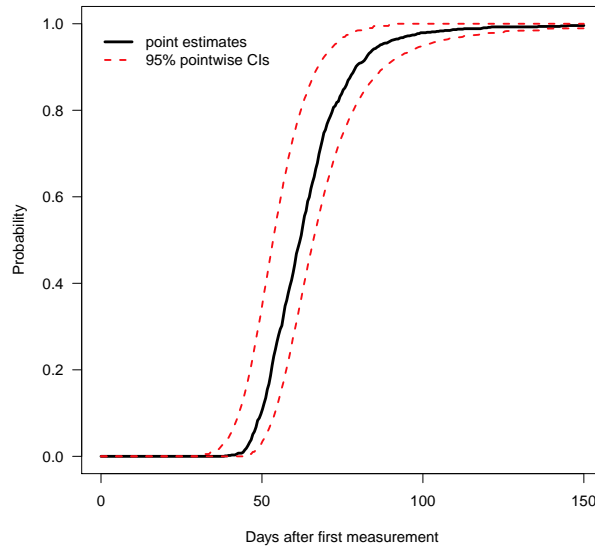
Figure 6: The estimated cdf and corresponding 95% pointwise CIs for a population with units starting randomly from day 161 to day 190.
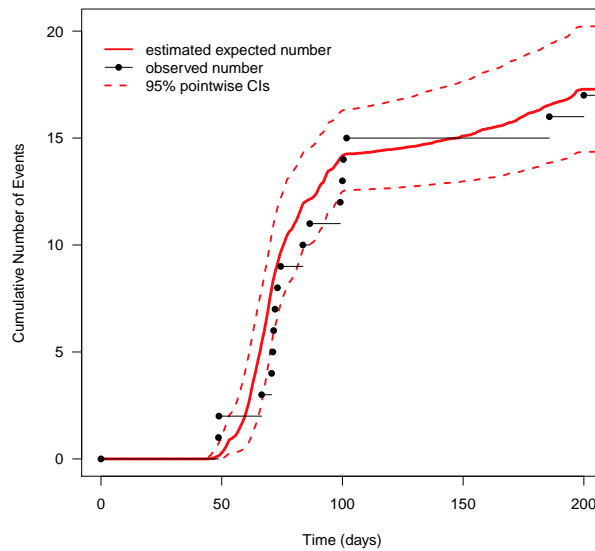

Figure 7: Estimated expected number of failures and corresponding 95% pointwise CIs versus the observed number of failures as a function of time for the 36 specimens in the outdoor weathering data.
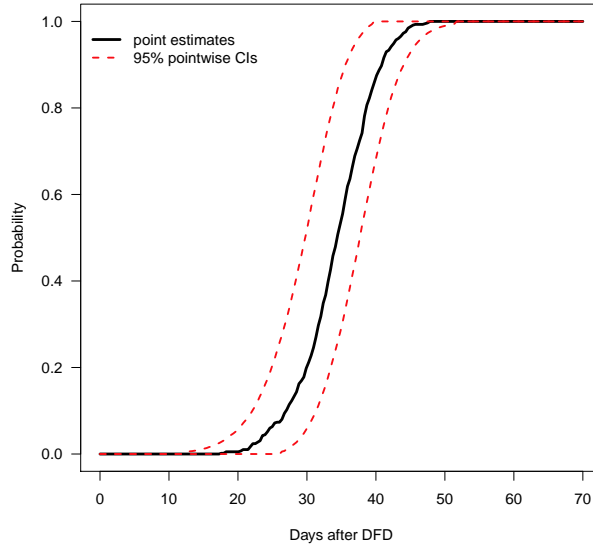
Figure 8: The estimated conditional cdf of remaining life and corresponding 95% pointwise CIs for unit G18-10.

158 days. Conditional on the observed degradation path and the covariate history for this unit, we can compute the estimated cdf of remaining life for this unit. Figure 8 shows the estimated conditional cdf for unit G18-10 and the corresponding 95% pointwise CIs. The results in Figure 8 show that the remaining life of this unit is roughly with the range of 20 days to 50 days.

6   Concluding Remarks and Areas for Future Research

Motivated by the increasing availability of dynamic covariate information being acquired by systems operating in the field and the needs to predict future performance of these systems, in this paper we develop a class of models and methods for using such data. We illustrate these methods by the outdoor weathering data. We use flexible general path models with individual random components to describe unit-to-unit variability in the degradation data. Parametric models are used to model the covariate processes. We develop algorithms to compute an estimate for the failure-time distribution induced by the underlying degradation model. We use the outdoor weathering data to illustrate the modeling process and the estimation of the failure-time distribution functions.

Although the NIST outdoor weathering data was our motivating example, the methods developed in this paper can have broad applications for many products used in highly variable

environments and/or subject to time-varying usages. For example, the degradation of LED power output is mainly due to usage that can be time varying. The corrosion of crude oil transportation pipeline is subject to the outdoor environments and the characteristics of the compounds flowing in the pipeline. Damage done to structures in aircraft will depend on the number of takeoff-landing cycles and other stresses encountered during operation. Also, the degradation of photovoltaic arrays can be caused by both the time-varying usage and the outdoor environments. Thus there are tremendous opportunities to apply the method developed in the paper.

For weathering applications, in the past decades, many solar UV monitoring sites have been established at different geographical locations within the United States and worldwide (e.g., as described in Kaetzel 2001). The solar UV spectrum and intensity, as well as temperature and relative humidity are recorded at high resolution. Such information can be used for prediction for the lifetime of products that are subject to degradation. When the covariate information is from different locations, spatial correlations may need to be considered for the model to predict the covariates for a population. Spatial data modeling techniques can be applied. In other applications, where the product is not exposed to sunlight or other weather variables, our models can still be used to model degradation as a function of other variables like load or amount of use.

The additive model for degradation paths proposed in this paper is equivalent to linear degradation path when the covariates are time invariant. In the future, it will be useful to consider nonlinear degradation paths. That is the degradation path $\mathcal{D}(t) = g\{D[t; \boldsymbol{x}(t)] + R(t; w)\}$ where $g(\cdot)$ is a nonlinear function that depends on some unknown parameters. The estimation for such a model will, however, be challenging.

A   Nonparametric Residual Bootstrap with Adjustment

In this appendix, we described the nonparametric residual bootstrap method for the linear mixed-effects model used in Section 3.4. The method was proposed by Carpenter, Goldstein, and Rasbash (2003) and we customized it for the model in this paper. As described in Carpenter, Goldstein, and Rasbash (2003), the sample variance-covariance matrix of the estimated random effects is different from the variance-covariance matrix of the random effect. Resampling the estimated random effects without appropriate adjustment will result in bias in estimate of the variance of the random effect. Thus adjustment is needed. The steps of the bootstrap algorithm are described as follows.

Algorithm 3:

1. Compute the parametric estimates for model (7) using **Algorithm 1** and then obtain the estimated residuals $\widehat{\varepsilon}_i(t_{ij}), i = 1 \ldots, n, j = 1, \ldots, n_i$ and estimated random effects $\widehat{w}_i = (\widehat{w}_{0i}, \widehat{w}_{1i})', i = 1, \ldots, n$. Let W be an $n \times 2$ matrix and the ith row of W is $\widehat{w}_i$.

2. Adjust the estimated random effects by a linear transformation. The basically idea is to match the sample variance-covariance matrix for the estimated random effects to the estimated variance-covariance of the random effect (i.e., $\widehat{\Sigma}_w$). In particular, we need to find A such that $A'SA = \widehat{\Sigma}_w$ where $S = W'W/n$. By Cholesky decomposition in terms of lower triangular matrix, we obtain $S = L_1 L_1'$ and $\widehat{\Sigma}_w = L_2 L_2'$. Take $A = L_2 L_1^{-1}$ and the transformed random effects are obtained by WA.

3. Sample with replacement from $\widehat{\varepsilon}_i(t_{ij})$ and transformed $\widehat{w}_i$ to obtain $\varepsilon_i^*(t_{ij})$, w_i^*. Note that we sample the row vectors of those transformed $\widehat{w}_i$ with replacement instead of individual elements.

4. Compute the bootstrap version of the data by

$$y_i^*(t_{ij}) = \widehat{\beta}_0 + \sum_{l=1}^{p} \sum_{q=1}^{Q_l} B_{lq}(t_{ij})\widehat{\beta}_{lq} + w_{0i}^* + w_{1i}^* t_{ij} + \varepsilon_i^*(t_{ij}).$$

5. Re-fit the model to the bootstrap version of the data using **Algorithm 1** to obtain the bootstrap estimates of model parameters.

6. Repeat steps 3 to 5 B times to obtain B sets of bootstrap parameter estimates for inference. The number of repeats was $B = 10000$ for the results in Section 3.4.

References

Bagdonavičius, V., I. Masiulaitytė, and M. S. Nikulin (2010). Reliability estimation from failure-degradation data with covariates. In M. S. Nikulin, N. Limnios, N. Balakrishnan, W. Kahle, and C. Huber-Carol (Eds.), *Advances in Degradation Modeling: Applications to Reliability, Survival Analysis, and Finance*, Chapter 18. Boston: Birkhäuser.

Bagdonavičius, V. and M. S. Nikulin (2001a). *Accelerated Life Models: Modeling and Statistical Analysis*. Boca Raton, FL: Chapman & Hall/CRC.

Bagdonavičius, V. and M. S. Nikulin (2001b). Estimation in degradation models with explanatory variables. *Lifetime Data Analysis 7*, 85–103.

Campbell, S. D. and F. X. Diebold (2005). Weather forecasting for weather derivatives. *Journal of the American Statistical Association 100*, 6–16.

Carpenter, J. R., H. Goldstein, and J. Rasbash (2003). A novel bootstrap procedure for assessing the relationship between class size and achievement. *Applied Statistics 52*, 431–443.

Davidov, O. and S. Rosen (2011). Constrained inference in mixed-effects models for longitudinal data with application to hearing loss. *Biostatistics 12*, 327–340.

Escobar, L. A., W. Q. Meeker, D. L. Kugler, and L. L. Kramer (2003). Accelerated destructive degradation tests: Data, models, and analysis. In B. H. Lindqvist and K. A. Doksum (Eds.), *Mathematical and Statistical Methods in Reliability*. Singapore: World Scientific Publishing Company.

Fraser, D. A. S. and H. Massam (1989). A mixed primal-dual bases algorithm for regression under inequality constraints. Application to concave regression. *Scandinavian Journal of Statistics 16*, 65–74.

Gebraeel, N. and J. Pan (2008). Prognostic degradation models for computing and updating residual life distributions in a time-varing environment. *IEEE Transactions on Reliability 57*, 539–550.

Gu, X., B. Dickens, D. Stanley, W. E. Byrd, T. Nguyen, I. Vaca-Trigo, W. Q. Meeker, J. W. Chin, and J. W. Martin (2009). Linking accelerating laboratory test with outdoor performance results for a model epoxy coating system. In J. Martin, R. A. Ryntz, J. Chin, and R. A. Dickie (Eds.), *Service Life Prediction of Polymeric Materials*. NY: New York: Springer.

Joseph, V. R. and I. Yu (2006). Reliability improvement experiments with degradation data. *IEEE Transactions on Reliability 55*, 149–157.

Kaetzel, L. J. (2001). Data management and a spectral solar UV network. In J. W. Martin and D. R. Bauer (Eds.), *Service Life Prediction Methodologies and Metrologies*, American Chemical Society Symposium Series 805, Chapter 5. New York: Oxford Press.

Lawless, J. F. and M. Crowder (2004). Covariates and random effects in a gamma process model with application to degradation and failure. *Lifetime Data Analysis 10*, 213–227.

Liu, Q. and D. A. Pierce (1994). A note on Gauss-Hermite quadrature. *Biometrika 81*, 624–629.

Lu, C. J. and W. Q. Meeker (1993). Using degradation measures to estimate a time-to-failure distribution. *Technometrics 34*, 161–174.

Lütkepohl, H. (2005). *New Introduction to Multiple Time Series Analysis* (Second ed.). Berlin: Springer-Verlag.

Meeker, W. Q. and L. A. Escobar (1998). *Statistical Methods for Reliability Data.* New York: John Wiley & Sons, Inc.

Meeker, W. Q., L. A. Escobar, and C. J. Lu (1998). Accelerated degradation tests: modeling and analysis. *Technometrics 40*, 89–99.

Meyer, M. C. (2008). Inference using shape-restricted regression splines. *The Annals of Applied Statistics 2*, 1013–1033.

Morris, J. S. (2002). The BLUPs are not "best" when it comes to bootstrapping. *Statistics & Probability Letters 56*, 425–430.

Nelson, W. (2001). Prediction of field reliability of units, each under differing dynamic stresses, from accelerated test data. In N. Balakrishnan and C. R. Rao (Eds.), *Handbook of Statistics 20: Advances in Reliability*, Chapter IX. Amsterdam: North-Holland.

Park, C. and W. J. Padgett (2006). Stochastic degradation models with several accelerating variables. *IEEE Transactions on Reliability 55*, 379–390.

R (2012). *The R Project for Statistical Computing.* http://www.r-project.org/.

Ramsay, J. O. (1988). Monotone regression splines in action. *Statistical Science 3*, 425–441.

Reinsel, G. C. (2003). *Elements of Multivariate Time Series Analysis* (2nd ed.). New York: Springer-Verlag.

Self, S. G. and K.-Y. Liang (1987). Asymptotic properlies of maximum likelihood estimators and likelihood ratio tests under nonstandard conditions. *Journal of the American Statistical Association 82*, 605–610.

Singpurwalla, N. D. (1995). Survival in dynamic environments. *Statistical Science 10*, 86–103.

Zhou, R. R., N. Serban, and N. Gebraeel (2011). Degradation modeling applied to residual lifetime prediction using functional data analysis. *The Annals of Applied Statistics 5*, 1586–1610.